

## Research Article

# Analysis of Iterative Erasure Insertion and Decoding of FH/MFSK Systems without Channel State Information

Jinsoo Park <sup>1</sup>, Gangsan Kim,<sup>1</sup> Hong-Yeop Song <sup>1</sup>, Chanki Kim <sup>2</sup>,  
Jong-Seon No,<sup>2</sup> and Suil Kim<sup>3</sup>

<sup>1</sup>Department of Electrical and Electronic Engineering, Yonsei University, Seoul 120-749, Republic of Korea

<sup>2</sup>Department of Electrical and Computer Engineering, Seoul National University, Seoul 151-742, Republic of Korea

<sup>3</sup>Agency for Defense Development, Daejeon 305-600, Republic of Korea

Correspondence should be addressed to Hong-Yeop Song; [hysong@yonsei.ac.kr](mailto:hysong@yonsei.ac.kr)

Received 4 September 2017; Accepted 27 December 2017; Published 24 January 2018

Academic Editor: Kiseon Kim

Copyright © 2018 Jinsoo Park et al. This is an open access article distributed under the Creative Commons Attribution License, which permits unrestricted use, distribution, and reproduction in any medium, provided the original work is properly cited.

We analyze the symbol measures for iterative erasure insertion and decoding of a Reed-Solomon coded SFH/MFSK system over jamming channels. In contrast to conventional erasure insertion schemes, iterative schemes do not require any preoptimized threshold or channel state information at the receiver. We confirm the performance improvement using a generalized minimum distance (GMD) decoding method with three different symbol measures. To analyze performance, we propose a new analysis framework considering the “trapped-error” probability. From analysis and the simulation results, we show that ratio-based GMD decoding has the best performance among the one-dimensional iterative erasure insertion and decoding schemes.

## 1. Introduction

To mitigate the threat of jamming attacks, Reed-Solomon (RS) coded frequency-hopping spread-spectrum systems with frequency shift keying (FSK) have been widely applied to military communication systems [1]. Although these systems can reduce the effect of jamming attacks, some signals are corrupted when the jamming signal collides with the hopping frequency. To recover information from the contaminated signals, various channel codes have been applied with an interleaver [1]. In many previous studies [2–11], erasure insertion schemes with an error and erasure decoder have been used to increase system reliability under this kind of jamming. The main aim of erasure insertion is to erase the corrupted received symbols (or dwells) using the threshold test. In most cases, the receiver should select an optimal threshold based on the system settings and the channel state at the time. If the receiver knows perfect channel state information, the performance can be improved using soft-decision-based soft-decoding algorithms [12–18]. However, it is very difficult to estimate the channel state information at the receiver (CSIR) when the channel is jammed [7].

In this paper, we consider an erasure insertion scheme that does not require any CSIR. Using appropriate symbol measures, we can improve the performance using several well-known iterative decoding algorithms [19–22]. These algorithms require the order of reliability of the received symbols, not exact soft measure of the symbols. Specially, we consider “output,” “ratio,” and “sum” measures using generalized minimum distance (GMD) decoding. Some other decoding algorithms, such as [23], can be applied after the iterative erasure insertion, but it is out of our scope. This iterative erasure insertion and decoding scheme does not guarantee independent processing of the received symbols; therefore, we propose a new analysis framework in terms of trapped-error probability. Finally, we confirm that the ratio measure works best and its concatenated scheme with another measure improves the performance when the jamming signal is strong. In [8], the authors proposed another iterative erasure insertion and decoding scheme, but they considered a partial-band jamming channel and a standard bounded-distance decoding. In this paper, we cover the partial-band and partial-time jamming, and we exploit GMD decoding, not a bounded-distance decoding.

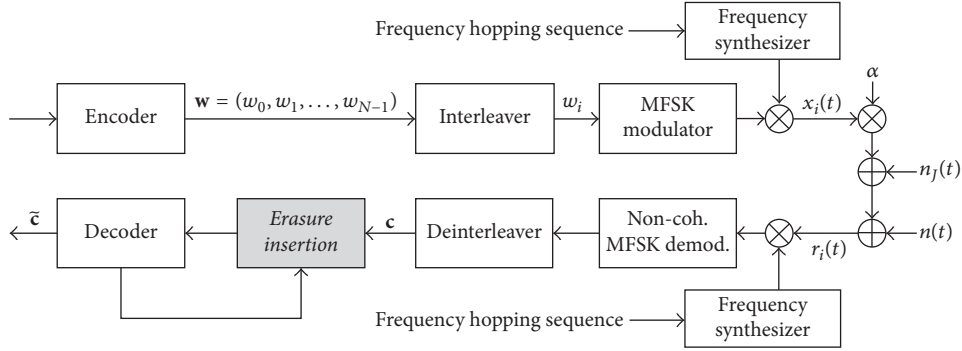


FIGURE 1: System block diagram with erasure insertion component.

This paper is organized as follows. In Section 2, we describe the system model. In Section 3, we review several conventional erasure insertion schemes and describe the iterative erasure insertion and decoding schemes. In Section 4, the trapped-error probability of the measures is derived. In Section 5, we compare the trapped-error probabilities and confirm the performances using computer simulations. Finally, concluding remarks are given in Section 6.

## 2. System Model

In this paper, we consider the RS coded slow frequency-hopping  $M$ -ary FSK system over a partial-band (or partial-time) jamming channel. At the transmitter,  $K$  information symbols are encoded by rate  $K/N$  RS encoder, where  $N$  is the number of codeword symbols. It is well known that  $(N, K)$  RS codes can recover the received word if  $u + 2v < N - K + 1$  and bounded-distance decoding is applied, where  $u$  and  $v$  are the number of erasures and errors in the received word, respectively. The encoded codeword is represented by

$$\mathbf{w} = (w_0, w_1, \dots, w_{N-1}), \quad (1)$$

where  $w_i, i \in \{0, \dots, N - 1\}$ , is the  $i$ th codeword symbol. We assume that an  $M$ -ary FSK modulated symbol represents the single corresponding RS codeword symbol over  $GF(M)$ , where  $M = 2^b$  and  $b$  is a positive integer. Furthermore, we assume  $N = M - 1$ , because the conventional RS codes over  $GF(M)$  have length  $N = M - 1$ .

The system model is shown in Figure 1. The jamming signal is inserted into the frequency domain with fraction (jamming duty ratio)  $\rho$ , which is the ratio of the jamming signal bandwidth to the spread-spectrum bandwidth. We assume that the partial-band jamming signal has a Gaussian distribution with zero-mean and  $N_j/2\rho = \sigma_j^2$  power spectral density in the jamming bandwidth. In the figure,  $\alpha$  represents the channel coefficients of the transmitter-receiver channel. If the transmitter-receiver channel is modeled as an additive white Gaussian noise (AWGN) channel, then the channel coefficient is set to  $\alpha = 1$ . The noise signal is modeled by a Gaussian distribution with zero-mean and  $N_0/2 = \sigma_N^2$  power spectral density over the entire frequency domain.

Throughout this paper, we assume an ideal interleaver. From this assumption, every RS codeword symbol is transmitted over a different frequency hop, and these symbols are independently interfered with the jamming signal with probability  $\rho$ . This assumption (and our result) covers every case such that the received symbol is independently interfered with probability  $\rho$ , such as partial-band and partial-time jamming. Based on this assumption, we will discuss the symbols that are independently jammed with probability  $\rho$ .

Let

$$x_i(t) = \sqrt{\frac{2E_s}{T}} \cos(2\pi(f_h + f_j)t) \quad (2)$$

be a general form of the transmitted signal, where  $E_s$ ,  $T$ , and  $f_h$  are symbol energy, symbol duration, and a selected hopping frequency, respectively. The orthogonal frequency  $f_j = j\Delta f$ , for  $j \in \{0, \dots, M - 1\}$ , is the selected frequency associated with  $w_i$ , where  $\Delta f = 1/T$ . If the transmitted symbol is contaminated by a jamming signal, the  $i$ th received signal  $r_i(t)$  is expressed as

$$r_i(t) = \alpha \sqrt{\frac{2E_s}{T}} \cos(2\pi(f_h + f_j)t + \theta) + n_j(t) + n(t), \quad (3)$$

where  $n_j(t)$  and  $n(t)$  are the jamming signal and Gaussian noise, respectively. A uniform random phase is denoted by  $\theta$ . For the unjammed case,  $n_j(t) = 0$ . Without loss of generality, we assume that  $E_s = 1$ .

The non-coherent MFSK demodulator calculates  $y_{i,j}$  for the  $i$ th symbol of the codeword and  $j$ th MFSK tone as follows [24]:

$$y_{i,j} = \left( \int_0^T r_i(t) \cos(2\pi(f_h + f_j)t) dt \right)^2 + \left( \int_0^T r_i(t) \sin(2\pi(f_h + f_j)t) dt \right)^2. \quad (4)$$

The symbol index  $i$  can be omitted if it is obvious based on the context. Thus,  $y_j$  denotes the value  $y_{i,j}$  in this case. After deinterleaving, all of the values of  $y_{i,j}$ , for  $0 \leq i \leq N - 1$  and  $0 \leq j \leq M - 1$ , are input to "erasure insertion." This block erases several symbols with a selected rule, which will be described in Section 3.

### 3. Erasure Insertion Schemes

#### 3.1. Overview of Erasure Insertion Schemes

**3.1.1. Conventional Schemes.** Next, we briefly introduce the three conventional erasure insertion schemes: the ratio threshold test (RTT), the output threshold test (OTT), and the maximum output-ratio threshold test (MO-RTT) [4–7, 25]. Let  $\max\{\cdot\}$  and  $\max'\{\cdot\}$  represent the first and second maximum values of a given set, respectively. For each  $i$  from 0 to  $N - 1$ , the  $i$ th received symbol is erased by RTT if  $\max'_j\{y_j\}/\max_j\{y_j\} > \lambda$ , where  $\lambda$  is a given threshold. OTT erases the symbol if  $\max_j\{y_j\} > \tau$ , for a given threshold  $\tau$ . Sometimes, the OTT rule is applied as  $\max_j\{y_j\} < \tau$  [6]; however, this reversed inequality is not considered in this paper. We note that the conventional RTT and OTT are one-dimensional erasure insertion schemes, because the decision is made using a single measure. On the other hand, MO-RTT is a two-dimensional erasure insertion scheme, combining OTT and RTT. MO-RTT generally exhibits better performance than RTT or OTT with their optimal thresholds. Before we discuss the problems of conventional schemes, we introduce a new threshold test scheme, that is, sum-based threshold test (STT). This test erases the symbol if  $\sum_{j=0}^{M-1} y_j > \mu$ , where  $\mu$  is a given threshold.

Threshold test-based conventional schemes have used the one-time erasure insertion and the bounded-distance decoding with preoptimized thresholds. The optimum thresholds depend on the channel state; therefore, the receiver should know the channel state information at the time. Because of the difficulty of obtaining perfect CSIR over jamming channels, we consider the iterative erasure insertion scheme, which does not require any CSIR.

**3.1.2. Iterative Erasure Insertion and Decoding Schemes.** To increase the error correction capability of RS codes, many iterative decoding algorithms have been proposed [19–23]. For an unjammed channel, we can estimate the channel state information using various techniques. Thereafter, we can apply various decoding algorithms. However, if the jamming signal exists and CSIR is not available, we must address the jamming attack without CSIR. To use the iterative decoding algorithms without CSIR, we will consider a simplified version of the GMD decoding algorithm [26], as an example. The main idea of GMD decoding is iterative decoding trials with erasures. During each iteration, GMD decoding erases the least reliable symbol and attempts an error and erasure decoding. In this paper, we use the symbol measures ratio ( $\max'_j\{y_j\}/\max_j\{y_j\}$ ), output ( $\max_j\{y_j\}$ ), and sum ( $\sum_{j=0}^{M-1} y_j$ ), for the GMD decoding algorithm. These schemes will be called ratio-based GMD (R-GMD), output-based GMD (O-GMD), and sum-based GMD (S-GMD) decoding, respectively. Note that the three measures are calculated without CSIR.

In Algorithm 1, the one-dimensional GMD algorithm is described using the three measures. Here,  $i$  is the index of the codeword symbol and  $j$  is the index of  $M$  detectors of the MFSK demodulator. Initially, the receiver decides that  $c_i =$

$\arg \max_j\{y_{i,j}\}$  for each  $i$  from 0 to  $N - 1$ . In the beginning of while loop, the decoder attempts to recover the transmit word  $\mathbf{w}$  in (1) from  $\mathbf{c}$  with error-only decoding. This step prevents performance degradation when there is no jamming signal. Additionally, we will not consider the undetected errors of the decoded codeword, because they seldom occur [27]. If the decoder declares a decoding failure, it erases the most suspicious (likely to have been jammed) symbol  $c_{i_{\max}}$  and replaces it with an erasure  $\epsilon$ , where  $i_{\max}$  is determined by the selected decision rule. For each measure,  $i_{\max}$  is determined as follows:

Ratio measure:

$$i_{\max} = \arg \max_{i \notin E} \left\{ \frac{\max'_j \{y_{i,j}\}}{\max_j \{y_{i,j}\}} \right\}. \quad (5)$$

Output measure:

$$i_{\max} = \arg \max_{i \notin E} \{y_{i,j}\}. \quad (6)$$

Sum measure:

$$i_{\max} = \arg \max_{i \notin E} \left\{ \sum_{j=0}^{M-1} y_{i,j} \right\}. \quad (7)$$

After  $i_{\max}$  is determined, it is added to  $E$ , which is the current set of erased symbol indices. Then, error and erasure decoding is applied. As we noted in Section 2,  $(N, K)$  RS codes can correct  $u$  erasures and  $v$  errors if  $u + 2v < N - K + 1$  is satisfied. If the decoding is successful, then the erasure insertion loop is terminated and the decoded codeword becomes the output  $\tilde{\mathbf{c}}$ . Otherwise, the algorithm continues to the second iteration of the while loop. In the second iteration and thereafter, all of the previously erased symbol indices ( $E$ ) are maintained and  $i_{\max}$  is determined over all the unerased indices. This iteration runs successively until the decoding succeeds or the number of erased symbols is the same as the number of parity symbols, that is,  $|E| = N - K$ . The while loop in Algorithm 1 is described by the feedback loop in Figure 1. We note that this iterative erasure insertion and GMD decoding algorithm runs independently for each codeword and does not make comparisons with any preoptimized threshold. Furthermore, if the conventional erasure insertion scheme can recover the codeword, then the corresponding iterative scheme can recover the codeword.

**3.2. Two-Dimensional Schemes.** We introduced the MO-RTT at the beginning of Section 3 which has two-dimensional measures, the joint threshold tests of OTT and RTT. To exploit the diversity of multiple measures, various combinations of iterative schemes with some different measures are considered. In this paper, however, we will focus only on serial concatenation of R-GMD decoding and S-GMD decoding, called ratio-to-sum-based GMD (RS-GMD) decoding. First, RS-GMD decoder runs R-GMD decoding. If R-GMD decoding fails to decode with  $|E| = N - K + 1$ , then the receiver

```

Initialize:
  Decide a vector  $\mathbf{c}$  by  $c_i = \arg \max_j \{y_{i,j}\}$ ,  $0 \leq i \leq N - 1$ 
  Set  $E = \emptyset$ 
while  $|E| \leq N - K$  do
  Try to error-and-erasure decode  $\mathbf{c}$ 
  if decoding success then
     $\tilde{\mathbf{c}}$  is the decoded codeword
    Break while loop
  else if decoding fail then
    Case: Measure
    ratio:  $i_{\max} = \arg \max_{i \notin E} \{\max'_j \{y_{i,j}\} / \max_j \{y_{i,j}\}\}$ 
    output:  $i_{\max} = \arg \max_{i \notin E} \{y_{i,j}\}$ 
    sum:  $i_{\max} = \arg \max_{i \notin E} \{\sum_{j=0}^{M-1} y_{i,j}\}$ 
    Erase  $i_{\max}$ th codeword symbols, i.e. set  $c_{i_{\max}} = \epsilon$ 
     $E \leftarrow E \cup \{i_{\max}\}$ 
  end if
end while
if  $|E| \leq N - K$  then
  Decoding success
  Output =  $\tilde{\mathbf{c}}$ 
else ( $|E| = N - K + 1$ )
  Decoding renounce
end if

```

ALGORITHM 1: Iterative erasure insertion and GMD decoding.

TABLE 1: Thresholds  $z_p$  of the three measures where  $M = 4$ ,  $p = 0.1$ ,  $\rho = 0.1$ , and  $E_b/N_0 = 5$  dB over AWGN and partial-band jamming channels.

$E_b/N_j$ (dB)	-10	-5	0	5	10	15	20
$z_p$ of R	0.722	0.722	0.721	0.719	0.712	0.695	0.671
$z_p$ of O	4.123	3.625	3.158	2.462	2.103	1.993	1.961
$z_p$ of S	4.824	4.377	4.438	3.400	2.869	2.623	2.536

runs S-GMD decoding again from the beginning. We will show the performance improvement of RS-GMD decoding as compared to the performance of MO-RTT over various channel situations in Section 5. In Table 2, the conventional, iterative, and two-dimensional schemes are classified into the four types of measures.

#### 4. Trapped-Error Probability

For the conventional erasure insertion schemes, that is, RTT, OTT, and MO-RTT, the error and erasure probabilities are derived in [4–6]. And we have included the error and erasure probabilities of STT in the Appendix. Calculation of the error and erasure probabilities of a given symbol cannot be applied to the analysis of iterative schemes because the erasure insertion for one symbol is not independent of that for all other symbols. For performance analysis of the iterative schemes, we propose trapped-error probability analysis based on three measures: “ratio,” “output,” and “sum.” The trapped-error probability is a new and useful analysis framework to compare the quality of each measure.

Consider a received word  $\mathbf{c}$  of length  $N$ . Let  $Z_i$  be the measure of one symbol of  $\mathbf{c}$  for one of the three measures:  $Z_i =$

$\max'_j \{y_{i,j}\} / \max_j \{y_{i,j}\}$ ,  $Z_i = \max_j \{y_{i,j}\}$ , and  $Z_i = \sum_{j=0}^{M-1} y_{i,j}$  for ratio, output, and sum measures, respectively. First, we sort the received  $N$  symbols in descending order according to  $Z_i$  values that are calculated by one selected way (among the three kinds of measures). Let  $p$  denote the ratio of the window of interest to the length  $N$ . This ratio  $p$  should be chosen in the range of  $0 < p \leq (N - K)/N$ , because the  $(N, K)$  RS code can correct up to  $N - K$  erasures. Now, we count the number  $N_p$  of erroneous symbols in the upper most portion of  $pN$  symbols. Let  $N_t$  denote the total number of erroneous symbols in the received word  $\mathbf{c}$  of length  $N$ . Then, the trapped-error probability  $\Gamma$  is defined as the ratio between  $N_p$  and  $N_t$ :

$$\Gamma = \frac{N_p}{N_t}. \quad (8)$$

For example, let us assume that there are  $N = 100$  received symbols with a total of  $N_t = 15$  erroneous symbols. Let us assume that  $p = 0.1$ . And we consider the first 10 ( $=pN$ ) positions when all of the symbols are arranged in decreasing order of their corresponding measures. Let us assume that  $N_p = 8, 1$ , and 5 erroneous symbols are placed among these 10 positions for ratio, output, and sum measures, respectively.

Then, the trapped-error probabilities are  $\Gamma_R = 8/15$ ,  $\Gamma_O = 1/15$ , and  $\Gamma_S = 5/15$  for these respective measures. In this case, because the iterative schemes successively erase the symbols in decreasing order of each measure, the ratio measure works best for trapping (or identifying) the erroneous symbols, and the output measure works worst. For a given  $p$ , a larger trapped-error probability indicates better performance.

Without loss of generality, we assume that all-zero codeword  $\mathbf{w} = (0, \dots, 0)$  is transmitted; that is,  $f_0$  is selected for every symbol transmission. If a transmitted symbol does not interfere with the jamming signal and the AWGN channel is assumed, then the probability density functions (PDFs) of  $y_0$  and  $y_j$ ,  $j \in \{1, \dots, M-1\}$ , are derived as follows [24]:

$$\begin{aligned} g_{U,0}(y) &= \frac{1}{2\sigma_N^2} \exp\left(-\frac{y+1}{2\sigma_N^2}\right) I_0\left(\frac{\sqrt{y}}{\sigma_N^2}\right), \\ g_{U,j}(y) &= \frac{1}{2\sigma_N^2} \exp\left(-\frac{y}{2\sigma_N^2}\right). \end{aligned} \quad (9)$$

For the jammed case,

$$\begin{aligned} g_{J,0}(y) &= \frac{1}{2\sigma^2} \exp\left(-\frac{y+1}{2\sigma^2}\right) I_0\left(\frac{\sqrt{y}}{\sigma^2}\right), \\ g_{J,j}(y) &= \frac{1}{2\sigma^2} \exp\left(-\frac{y}{2\sigma^2}\right), \end{aligned} \quad (10)$$

where  $\sigma^2 = \sigma_J^2 + \sigma_N^2$  and  $I_0(\cdot)$  is the modified Bessel function of order zero.

If we assume Rayleigh fading channel without/partial-band jamming,  $g_{U,0}$  and  $g_{J,0}$  are changed as follows [28, 29]:

$$\begin{aligned} g_{U,0}(y) &= \frac{1}{2\sigma_N^2 + 1} \exp\left(-\frac{y}{2\sigma_N^2 + 1}\right), \\ g_{J,0}(y) &= \frac{1}{2\sigma^2 + 1} \exp\left(-\frac{y}{2\sigma^2 + 1}\right). \end{aligned} \quad (11)$$

Because  $g_{U,0}(y), \dots, g_{U,M-1}(y)$  and  $g_{J,0}(y), \dots, g_{J,M-1}(y)$  are independent variables, their joint PDFs can be represented as  $\prod_{j=0}^{M-1} g_{U,j}(y_j)$  and  $\prod_{j=0}^{M-1} g_{J,j}(y_j)$ , respectively. Their cumulative distribution functions (CDFs) are  $G_{U,j}(y_j)$  and  $G_{J,j}(y_j)$ , for  $j \in \{0, \dots, M-1\}$ , respectively.

Recall that  $Z_i$  is the measure of the symbol  $c_i$  for one of the three measures. For simplicity, we will omit the subscript  $i$ :  $Z = \max'_j \{y_j\} / \max_j \{y_j\}$ ,  $Z = \max_j \{y_j\}$ , or  $Z = \sum_{j=0}^{M-1} y_j$  for ratio, output, or sum measures, respectively. The CDF is simply denoted by  $F_Z(z)$ . Define  $H_0$  as a representation of the event of a raw symbol error, that is, the event where there exists at least one  $j \in \{1, \dots, M-1\}$  that satisfies  $y_0 < y_j$ .  $H_0$ 's complementary event is denoted by  $\bar{H}_0$ . Now, we consider the

conditional CDFs  $F_{Z|H}(z | H_0)$  and  $F_{Z|H}(z | \bar{H}_0)$ , where  $H$  is the discrete event variable  $H \in \{H_0, \bar{H}_0\}$ . Then,

$$\begin{aligned} F_Z(z) &= \Pr[H_0] F_{Z|H}(z | H_0) \\ &\quad + \Pr[\bar{H}_0] F_{Z|H}(z | \bar{H}_0), \\ f_Z(z) &= \Pr[H_0] f_{Z|H}(z | H_0) \\ &\quad + \Pr[\bar{H}_0] f_{Z|H}(z | \bar{H}_0), \end{aligned} \quad (12)$$

where  $f_s$  denote the corresponding PDFs.

Define  $z_p$  as the point that satisfies  $F_Z(z_p) = 1 - p$ .  $z_p$  is uniquely determined because  $F_Z(z)$  is monotonically increasing from 0 to 1. Then, the trapped-error probability  $\Gamma(z_p)$  can be defined as follows:

$$\Gamma(z_p) = \int_{z_p}^{\infty} f_{Z|H}(z | H_0) dz = 1 - F_{Z|H}(z_p | H_0). \quad (13)$$

Now, we will change (13) into a form involving  $\bar{H}_0$  instead of  $H_0$ , such that its computation can be easily performed. From (12), we observe that

$$\begin{aligned} F_Z(z_p) &= \Pr[H_0] F_{Z|H}(z_p | H_0) \\ &\quad + \Pr[\bar{H}_0] F_{Z|H}(z_p | \bar{H}_0) = 1 - p. \end{aligned} \quad (14)$$

Using (14), the trapped-error probability in (13) can be written as

$$\Gamma(z_p) = 1 - \frac{1 - p - \Pr[\bar{H}_0] F_{Z|H}(z_p | \bar{H}_0)}{\Pr[H_0]}. \quad (15)$$

Using the relation  $\Pr[H_0] + \Pr[\bar{H}_0] = 1$  and after some manipulation, we have the following:

$$\Gamma(z_p) = \frac{p - \Pr[\bar{H}_0] + \Pr[\bar{H}_0] F_{Z|H}(z_p | \bar{H}_0)}{1 - \Pr[\bar{H}_0]}. \quad (16)$$

Here,  $\Pr[\bar{H}_0]$  can be calculated as follows:

$$\begin{aligned} \Pr[\bar{H}_0] &= \Pr[y_0 > y_j, \forall j = 1, \dots, M-1] \\ &= \bar{\rho} \int_0^{\infty} \int_0^{y_0} \dots \int_0^{y_0} \prod_{j=0}^{M-1} g_{U,j}(y_j) dy_{M-1} \dots dy_0 \\ &\quad + \rho \int_0^{\infty} \int_0^{y_0} \dots \int_0^{y_0} \prod_{j=0}^{M-1} g_{J,j}(y_j) dy_{M-1} \dots dy_0 \\ &= \bar{\rho} \int_0^{\infty} g_{U,0}(y_0) (G_{U,1}(y_0))^{M-1} dy_0 \\ &\quad + \rho \int_0^{\infty} g_{J,0}(y_0) (G_{J,1}(y_0))^{M-1} dy_0, \end{aligned} \quad (17)$$

where  $\bar{\rho} = 1 - \rho$ .



Let us assume AWGN and a partial-band jamming channel. Using a binomial expansion and some calculations [30], (17) becomes

$$\begin{aligned} & \bar{\rho} e^{(-1/2\sigma_N^2)} \sum_{l=0}^{\infty} \sum_{m=0}^{M-1} \frac{(-1)^m}{(2\sigma_N^2)^l (m+1)^{l+1} l!} \binom{M-1}{m} \\ & + \rho e^{(-1/2\sigma^2)} \sum_{l=0}^{\infty} \sum_{m=0}^{M-1} \frac{(-1)^m}{(2\sigma^2)^l (m+1)^{l+1} l!} \binom{M-1}{m}. \end{aligned} \quad (18)$$

Similarly, for a Rayleigh fading and partial-band jamming channel, (17) becomes

$$\begin{aligned} & \bar{\rho} \sum_{m=0}^{M-1} \frac{2\sigma_N^2}{(2+2m)\sigma_N^2+m} (-1)^m \binom{M-1}{m} \\ & + \rho \sum_{m=0}^{M-1} \frac{2\sigma^2}{(2+2m)\sigma^2+m} (-1)^m \binom{M-1}{m}. \end{aligned} \quad (19)$$

Next, we compute  $F_{Z|H}(z_p | \bar{H}_0)$  as follows:

$$\begin{aligned} & F_{Z|H}(z_p | \bar{H}_0) \\ & = \frac{\Pr[Z < z_p, \gamma_0 > \gamma_{j'}, \forall j' = 1, \dots, M-1]}{\Pr[\bar{H}_0]}. \end{aligned} \quad (20)$$

Now, assume that we use the ratio measure. Then, the numerator of (20) becomes

$$\begin{aligned} & \Pr \left[ \frac{\max'_j \{y_j\}}{\max_j \{y_j\}} < z_p, \gamma_0 > \gamma_{j'}, \forall j' = 1, \dots, M-1 \right] \\ & = \Pr [\max'_j \{y_j\} < z_p \gamma_0] \\ & = \Pr [y_j < z_p \gamma_0, \forall j = 1, \dots, M-1] \\ & = \bar{\rho} \int_0^{\infty} \int_0^{z_p \gamma_0} \cdots \int_0^{z_p \gamma_0} \prod_{j=0}^{M-1} g_{U,j}(y_j) dy_{M-1} \cdots dy_0 \\ & + \rho \int_0^{\infty} \int_0^{z_p \gamma_0} \cdots \int_0^{z_p \gamma_0} \prod_{j=0}^{M-1} g_{J,j}(y_j) dy_{M-1} \cdots dy_0 \\ & = \bar{\rho} \int_0^{\infty} g_{U,0}(\gamma_0) (G_{U,1}(z_p \gamma_0))^{(M-1)} d\gamma_0 \\ & + \rho \int_0^{\infty} g_{J,0}(\gamma_0) (G_{J,1}(z_p \gamma_0))^{(M-1)} d\gamma_0. \end{aligned} \quad (21)$$

For AWGN and Rayleigh fading channels with partial-band jamming, (21) becomes (22) and (23), respectively.

$$\begin{aligned} & \bar{\rho} e^{(-1/2\sigma_N^2)} \sum_{l=0}^{\infty} \sum_{m=0}^{M-1} \frac{(-1)^m}{(2\sigma_N^2)^l (mz_p + 1)^{l+1} l!} \binom{M-1}{m} \\ & + \rho e^{(-1/2\sigma^2)} \sum_{l=0}^{\infty} \sum_{m=0}^{M-1} \frac{(-1)^m}{(2\sigma^2)^l (mz_p + 1)^{l+1} l!} \binom{M-1}{m}, \end{aligned} \quad (22)$$

$$\begin{aligned} & \bar{\rho} \sum_{m=0}^{M-1} \frac{2\sigma_N^2}{(2+2mz_p)\sigma_N^2+mz_p} (-1)^m \binom{M-1}{m} \\ & + \rho \sum_{m=0}^{M-1} \frac{2\sigma^2}{(2+2mz_p)\sigma^2+mz_p} (-1)^m \binom{M-1}{m}. \end{aligned} \quad (23)$$

For the output measure, the numerator of (20) becomes

$$\begin{aligned} & \Pr [\max_j \{y_j\} < z_p, \gamma_0 > \gamma_{j'}, \forall j' = 1, \dots, M-1] \\ & = \Pr [\gamma_0 < z_p, \gamma_0 > \gamma_j, \forall j = 1, \dots, M-1] \\ & = \bar{\rho} \int_0^{z_p} \int_0^{\gamma_0} \cdots \int_0^{\gamma_0} \prod_{j=0}^{M-1} g_{U,j}(y_j) dy_{M-1} \cdots dy_0 \\ & + \rho \int_0^{z_p} \int_0^{\gamma_0} \cdots \int_0^{\gamma_0} \prod_{j=0}^{M-1} g_{J,j}(y_j) dy_{M-1} \cdots dy_0 \\ & = \bar{\rho} \int_0^{z_p} g_{U,0}(\gamma_0) (G_{U,1}(\gamma_0))^{(M-1)} d\gamma_0 \\ & + \rho \int_0^{z_p} g_{J,0}(\gamma_0) (G_{J,1}(\gamma_0))^{(M-1)} d\gamma_0. \end{aligned} \quad (24)$$

With partial-band jamming, (24) becomes (25) and (26) for AWGN and Rayleigh fading channels, respectively.

$$\begin{aligned} & \bar{\rho} e^{(-1/2\sigma_N^2)} \sum_{l=0}^{\infty} \sum_{m=0}^{M-1} \frac{(-1)^m}{(2\sigma_N^2)^{2l+1} l!} \binom{M-1}{m} \\ & \cdot \left( \left( \frac{2\sigma_N^2}{m+1} \right)^{l+1} \right. \\ & \left. - e^{-(m+1)z_p/2\sigma_N^2} \sum_{n=0}^l \frac{z_p^n}{n!} \left( \frac{2\sigma_N^2}{m+1} \right)^{l+1-n} \right) \\ & + \rho e^{(-1/2\sigma^2)} \sum_{l=0}^{\infty} \sum_{m=0}^{M-1} \frac{(-1)^m}{(2\sigma^2)^{2l+1} l!} \binom{M-1}{m} \\ & \cdot \left( \left( \frac{2\sigma^2}{m+1} \right)^{l+1} \right. \\ & \left. - e^{-(m+1)z_p/2\sigma^2} \sum_{n=0}^l \frac{z_p^n}{n!} \left( \frac{2\sigma^2}{m+1} \right)^{l+1-n} \right), \end{aligned} \quad (25)$$

$$\begin{aligned}
& \bar{\rho} \sum_{m=0}^{M-1} \frac{2\sigma_N^2}{(2+2m)\sigma_N^2+m} (-1)^m \binom{M-1}{m} \cdot \left(1 - e^{-((2+2m)\sigma_N^2+m)/(4\sigma_N^4+2\sigma_N^2)z_p}\right) \\
& + \rho \sum_{m=0}^{M-1} \frac{2\sigma^2}{(2+2m)\sigma^2+m} \cdot (-1)^m \binom{M-1}{m} \left(1 - e^{-((2+2m)\sigma^2+m)/(4\sigma^4+2\sigma^2)z_p}\right). \tag{26}
\end{aligned}$$

For the sum measure, the numerator of (20) is given as (27). Actually, (27) is the same as (A.4) in the Appendix, where  $\mu = z_p$ . Using the derived equations, we can calculate the trapped-error probabilities of three measures.

$$\begin{aligned}
\Pr \left[ \sum_{j=0}^{M-1} y_{i,j} < z_p, y_0 > y_j, \forall j = 1, \dots, M-1 \right] &= \Pr \left[ y_0 < z_p, \right. \\
& \left. y_1 < \min(y_0, z_p - y_0), \dots, y_{M-1} < \min\left(y_0, z_p - \sum_{j=0}^{M-2} y_j\right) \right] \tag{27} \\
&= \bar{\rho} \int_0^{z_p} \int_0^{\min(y_0, z_p - y_0)} \dots \int_0^{\min(y_0, z_p - \sum_{j=0}^{M-2} y_j)} \prod_{j=0}^{M-1} g_{U,j}(y_j) dy_{M-1} \\
&\dots dy_0 \\
&+ \rho \int_0^{z_p} \int_0^{\min(y_0, z_p - y_0)} \dots \int_0^{\min(y_0, z_p - \sum_{j=0}^{M-2} y_j)} \prod_{j=0}^{M-1} g_{I,j}(y_j) dy_{M-1} \\
&\dots dy_0. \tag{28}
\end{aligned}$$

## 5. Simulation Results

**5.1. Trapped-Error Probabilities.** In this subsection, we confirm the trapped-error probability analysis over AWGN and Rayleigh fading channels with partial-band jamming. Let us assume 4-FSK,  $\rho = 0.1$ , and  $E_b/N_0 = 5$  dB for the AWGN channel and  $E_b/N_0 = 12$  dB for the Rayleigh fading channel. For the higher order of modulation, such as 32-FSK, which we will consider, (27) requires 32-dimensional integration; therefore, we select 4-FSK as an example. To calculate the probabilities  $\Gamma(z_p)$  for each measure, the input  $z_p$  should be obtained for the given set of system parameters. For this, we further assume that  $p = 0.1$  and  $0.2$  for AWGN and Rayleigh fading channels, respectively. As we described in Section 4, we found  $z_p$  values that satisfy  $F_z(z_p) = 1 - p$  using simulations. They are listed in Tables 1 and 3 for various  $E_b/N_j$ . R, O, and S refer to ratio, output, and sum, respectively. In the investigation, we transmitted  $10^5$  symbols for various channel states and calculated their ratio, output, and sum measures. We note that these trapped-error probabilities do not depend on a specific coding scheme, because these statistics are observed at the demodulator output without coding.

Figures 2 and 3 show the trapped-error probabilities of the three measures obtained using simulations and from (16) with the threshold values given in Tables 1 and 3. Solid and dashed lines indicate the probabilities obtained by simulation

TABLE 2: Class of erasure insertion schemes.

Measure	Threshold test	Iterative
Ratio	RTT	R-GMD
Output	OTT	O-GMD
Sum	STT	S-GMD
Two-dimensional	Ex: MO-RTT	Ex: RS-GMD

TABLE 3: Thresholds  $z_p$  of the three measures where  $M = 4$ ,  $p = 0.2$ ,  $\rho = 0.1$ , and  $E_b/N_0 = 12$  dB over Rayleigh fading and partial-band jamming channels.

$E_b/N_j$ (dB)	-5	0	5	10	15	20
$z_p$ of R	0.353	0.345	0.350	0.329	0.294	0.263
$z_p$ of O	2.271	2.233	2.053	1.765	1.681	1.660
$z_p$ of S	2.368	2.342	2.297	2.069	1.845	1.776

and (16), respectively. The cross, circle, and square marks represent  $\Gamma(z_p)$  values of ratio, output, and sum measures, respectively.

These two figures confirm that the simulation is exact enough to closely follow the theoretical result in (16). Specially,  $\Gamma_O$  in the analysis is almost the same as  $\Gamma_O$  in the simulation results. This result implies the correctness of our performance simulation.

In these figures, the trapped-error probability of the ratio measure is increased as SJR is increased; therefore, we predict that the R-GMD decoding will perform better than the other one-dimensional schemes at high SJR. Additionally, we predict that S-GMD decoding is better than O-GMD decoding in the middle SJR region. Recall that the higher the trapped-error probability, the better the performance. This observation shows the influence on the two-dimensional schemes, because the trapped-error probability affects the number of decoding trials. We will discuss it in the following simulation results.

**5.2. Performance over AWGN Channel.** Throughout performance simulations, we consider 32-ary FSK modulation with (31, 20) RS code over a field of size 32, an ideal interleaver, and a random hopping pattern. We first consider partial-band jamming (or partial-time jamming with the same  $\rho$ ) and AWGN channels. In this case,  $\alpha = 1$  in Figure 1. For Figures 4–7, the channel noise is fixed, as we used  $E_b/N_0 = 5$  dB. Various signals to jamming signal ratio  $E_b/N_j$  have been considered for the simulations.

In Figure 4, the performance of various erasure insertion schemes is plotted over the partial-band jamming channel with  $\rho = 0.1$ . The dashed line shows the baseline performance “Without EI,” which does not use any erasure insertion scheme. The unmarked solid line represents the performance of the MO-RTT, which is the conventional erasure insertion scheme. We note that the MO-RTT uses preoptimized thresholds and CSIR. To obtain the optimum thresholds for MO-RTT, we optimized the thresholds for  $E_b/N_j = 0 \sim 30$  dB with 10 dB steps. Solid lines with circle, square, cross, plus, and diamond marks represent the performance of output-based,

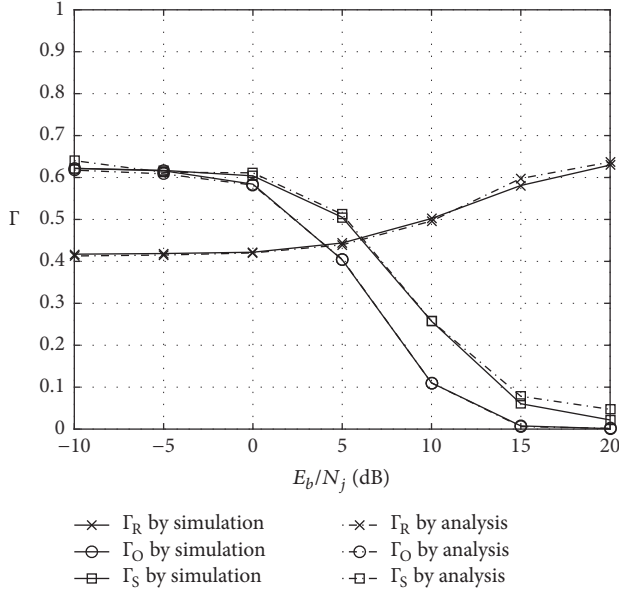


FIGURE 2: Trapped-error probabilities of ratio-based ( $\Gamma_R$ ), output-based ( $\Gamma_O$ ), and sum-based ( $\Gamma_S$ ) measures over partial-band jamming and AWGN channel.

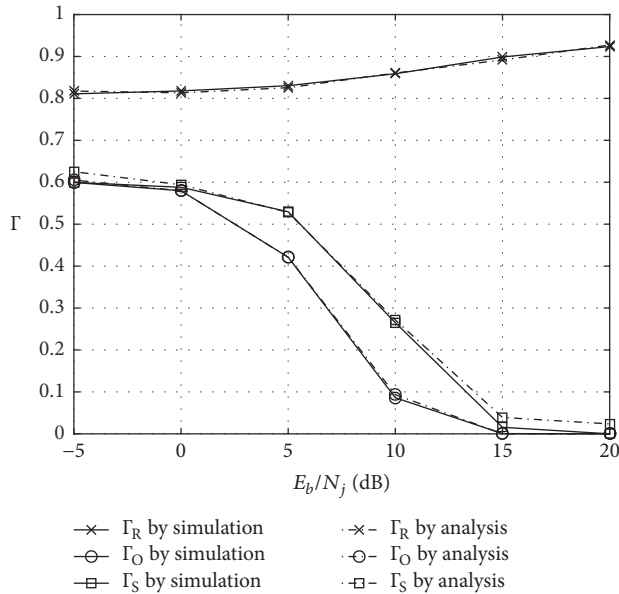


FIGURE 3: Trapped-error probabilities of ratio-based ( $\Gamma_R$ ), output-based ( $\Gamma_O$ ), and sum-based ( $\Gamma_S$ ) measures over partial-band jamming and Rayleigh channels.

sum-based, ratio-based, ratio-to-output-based, and ratio-to-sum-based GMD decoding, respectively. In this figure, we also present the performance using log-likelihood ratio (LLR) based GMD decoding as the triangle-marked line. This is the performance of a system with perfect CSIR, such as SNR, SJR, and the existence of a jamming signal. This LLR-GMD decoding iteratively erases the least reliable symbols based on LLR, as described in [19, 22, 26]. Because it is well known that MO-RTT exhibits better performance than OTT

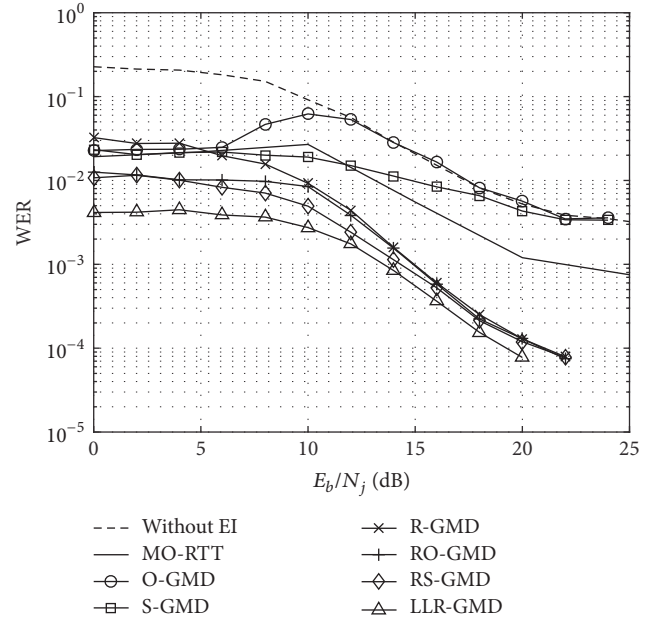


FIGURE 4: Performance of various erasure insertion schemes over partial-band jamming and AWGN channels with  $\rho = 0.1$  and  $E_b/N_0 = 5$  dB.

or RTT [5–7], the performances of OTT and RTT are omitted. Before discussing the simulation result, we note that RSO-GMD decoding, which serially exploits the three measures, has almost the same performance as RS-GMD decoding; therefore, we have also omitted it. From Figure 4, we make the following observations:

- (1) As we expect, LLR-GMD decoding with CSIR shows the best performance. We will focus on the performance gap between LLR-GMD decoding with CSIR and the other erasure insertion schemes without CSIR. To achieve  $\text{WER} = 10^{-4}$ , LLR-GMD decoding requires  $E_b/N_j = 19$  dB. The ratio-based GMD decoding and its two-dimensional schemes achieve the target WER at  $E_b/N_j = 21$  dB which is much closer than that of MO-RTT. Even if the jamming power is decreased as  $E_b/N_j = 25$  dB, the performance of MO-RTT is still far from  $\text{WER} = 10^{-4}$ . In the low SJR region, only the two two-dimensional iterative schemes can achieve  $\text{WER} = 10^{-2}$  without CSIR. We note that the one-dimensional iterative schemes and MO-RTT require  $E_b/N_j > 9$  dB to achieve  $\text{WER} = 10^{-2}$ .
- (2) The performance of RS-GMD decoding approaches that of LLR-GMD decoding, as SJR is increased. At  $E_b/N_j = 20$  dB, LLR-GMD decoding with perfect CSIR has 35% less WER than RS-GMD decoding. We note that this gap cannot be closed even if the jamming power is decreased.
- (3) When the jamming power is decreased, that is, the channel approaches the unjammed channel, the performance of R-GMD and RS-GMD decoding is



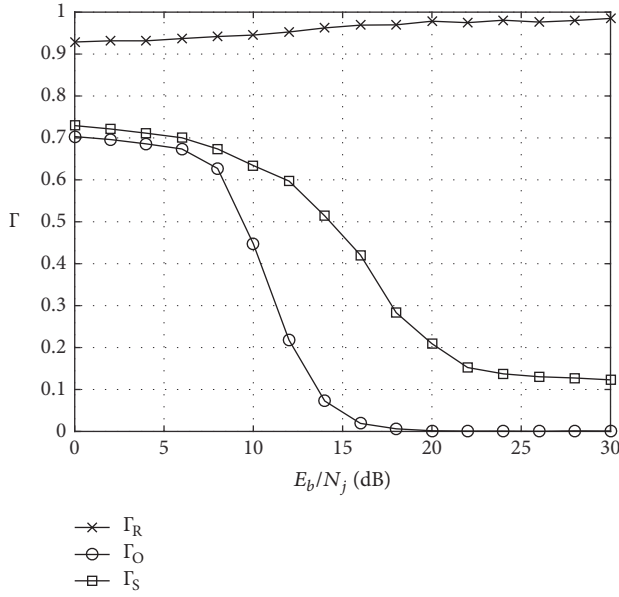


FIGURE 5: Trapped-error probability of various measures over partial-band jamming and AWGN channels with  $p = 0.3$ ,  $\rho = 0.1$ , and  $E_b/N_0 = 5$  dB.

still better than the performance of “Without EI” or MO-RTT. This implies that the iterative erasure insertion and decoding schemes do not decrease the performance if there are no jamming signals. Because of this, we do not need to detect the jamming signal.

In Figure 5, trapped-error probabilities of ratio, output, and sum measures are represented, which corresponds to Figure 4. To obtain the trapped-error probabilities, SJR and SNR were scaled based on the code rate  $20/31 = N/K$ , which is different from Section 5.1. We used  $p = 0.3$ , and the other parameters are the same as those used in Figure 4. In Figure 5,  $\Gamma_R$  is much larger than  $\Gamma_O$  and  $\Gamma_S$ . The values of  $\Gamma_R$  explain the good performance of R-GMD decoding. We find that  $\Gamma_O$  goes to  $< 1 - K/N \approx 0.3$  at  $E_b/N_j \approx 10$  dB. Any iterative scheme that has zero trapped-error probability at a given SJR has the same performance as the performance of “Without EI”. This result explains why O-GMD decoding has a performance degradation region near 10 dB, in Figure 4. Because the performance of O-GMD decoding rapidly approaches the performance of “Without EI”, its performance is degraded as SJR is increased. We note that the performance of S-GMD decoding slowly approaches the performance of “Without EI”; therefore, there is no performance degradation region.

The performance gain of the iterative schemes in Figure 4 cannot be obtained without drawbacks: the iterative schemes require more decoding trials. To investigate how many decoding trials are required, we determine the average number of decoding iterations of various iterative schemes via simulations. The results are shown in Figure 6. In fact, we simulated iterative schemes that erase one symbol during the first loop and then erase two symbols for each remaining loop, because this process does not decrease the performance, as described in [19]. In general, the average number of

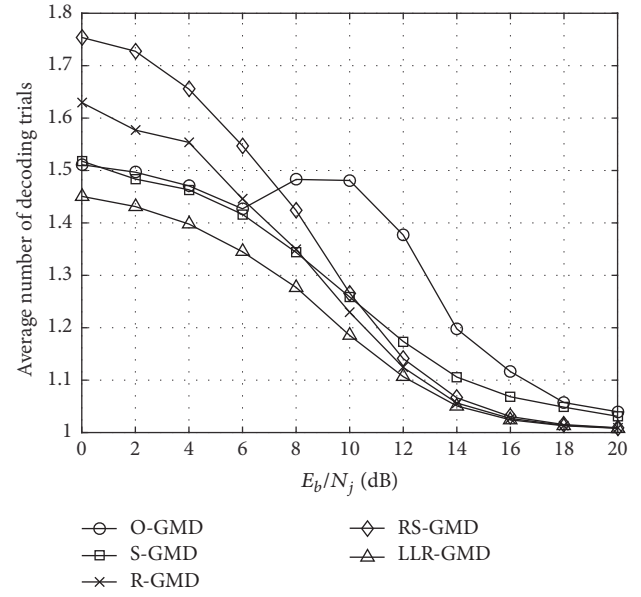


FIGURE 6: Average number of decoding iterations for various erasure insertion schemes over partial-band jamming and AWGN channels with  $\rho = 0.1$  and  $E_b/N_0 = 5$  dB.

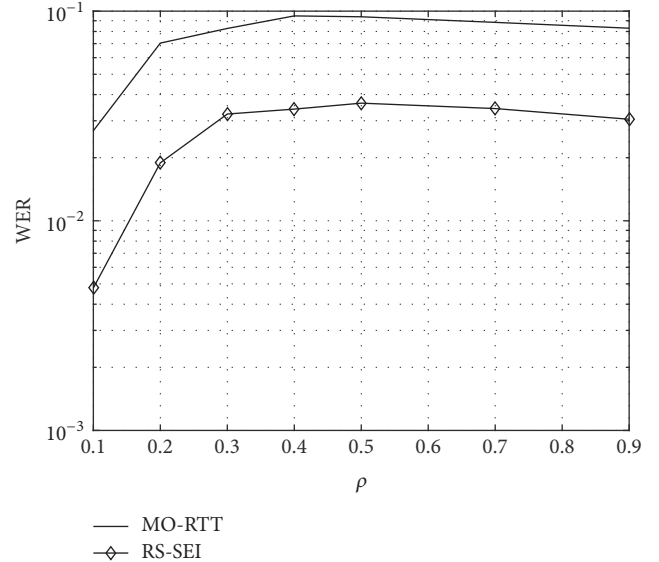


FIGURE 7: Performance comparison of MO-RTT and RS-GMD decoding scheme over partial-band jamming and AWGN channels with various values of  $\rho$ ,  $E_b/N_0 = 5$  dB and  $E_b/N_j = 10$  dB.

decoding trials decreases rapidly as SJR increases. At high SJR, most of the received words are completely decoded by a single trial of error-only decoding, which holds true because higher SJR implies that the environment becomes less and less hostile. For low SJR, the average decoding trial of RS-GMD decoding is approximately 1.75 (at  $E_b/N_j = 0$  dB), which decreases as SJR increases. This result indicates that the iterative erasure insertion and decoding scheme is practically implementable. We note that the trial number of O-GMD decoding is increased at approximately  $E_b/N_j \approx 10$  dB,

and that is consistent with the performance degradation of O-GMD decoding in Figures 4 and 5. Because O-GMD decoding could not accurately erase the erroneous symbols, the decoder has to try more decoding. Because of this result, we must use S-GMD decoding, instead of O-GMD decoding, for the two-dimensional scheme with R-GMD decoding. Now, recall the analysis results of Section 5.1. In Figure 2, we observed that the trapped-error probability of the ratio measure is increased as SJR is increased and that of the sum measure is decreased. For the case in which the trapped-error probabilities cross at the point of SJR, if we want to have fewer decodings at the higher SJR, then we must use R-GMD decoding first in RS-GMD decoding. If we want to have fewer decodings at the lower SJR, then S-GMD decoding should be applied first. In Figures 4 and 6, because we are considering the SJR region in which  $\Gamma_R > \Gamma_S$ , we have first exploited R-GMD decoding for RS-GMD decoding.

In Figure 7, the performances of MO-RTT and RS-GMD decoding are shown over a partial-band jamming and an AWGN channel with various jamming duty ratios  $\rho$  with fixed  $E_b/N_0 = 5$  dB and  $E_b/N_j = 10$  dB. For all values of  $\rho$ , RS-GMD decoding works much better than MO-RTT. We note that two erasure insertion schemes are more efficient for smaller  $\rho$  channels.

**5.3. Performance over Rayleigh Fading Channel.** Figure 8 shows the performance of various erasure insertion schemes over partial-band jamming and Rayleigh fading channel with  $\rho = 0.1$  and  $E_b/N_0 = 12$  dB. For each symbol transmission,  $\alpha$  in Figure 1 is realized by an i.i.d. Rayleigh distribution. We assume that fading coefficients are not known to the receiver, except for the system of MO-RTT.

In Figure 8, RS-GMD decoding exhibits better performance than MO-RTT, which is the same result as we found over the AWGN channel. For the same WER of  $10^{-3}$ , the jammer should spend 14 dB more  $N_j$ . The WER of ratio-based schemes (including two-dimensional schemes) approach  $10^{-4}$ . Unlike the results for an AWGN channel, R-GMD decoding is dominant and the contribution of S-GMD decoding is marginal. Therefore, we conclude that R-GMD decoding is sufficient for Rayleigh fading channels. Additionally, we present the performance of LLR-GMD decoding which knows perfect CSIR. As we discussed in Section 5.2, the performance of R-SEI approaches that of LLR-SEI and the gap is maintained for every SJR.

In Figure 9, the trapped-error probabilities of the measures are displayed over a Rayleigh fading channel with  $E_b/N_0 = 12$  dB. The other parameters are the same as those in Figure 5. In this figure, the trapped-error probability of the ratio measure is 1 in all SJR regions. In other words, R-GMD decoding is the best one-dimensional iterative scheme for the target system parameters. As we found for the other trapped-error probability results, the trapped-error probabilities of sum and output measures decrease as SJR increases. Where the trapped-error probabilities are lower than  $<1 - K/N \approx 0.3$ , that is,  $E_b/N_j = 10$  dB and 16 dB for output and sum, respectively, the performances of O-GMD and S-GMD decoding follow the performance of “Without EI”. As we

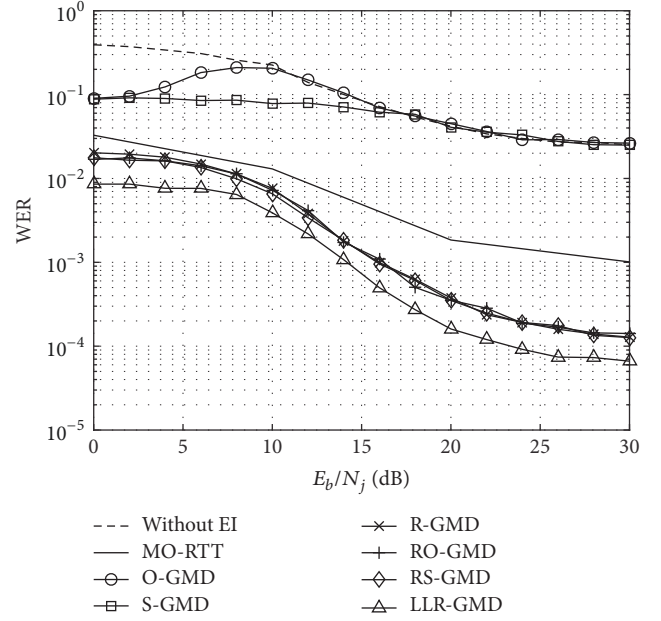


FIGURE 8: Performance of various erasure insertion schemes over a Rayleigh fading channel, where  $\rho = 0.1$  and  $E_b/N_0 = 12$  dB.

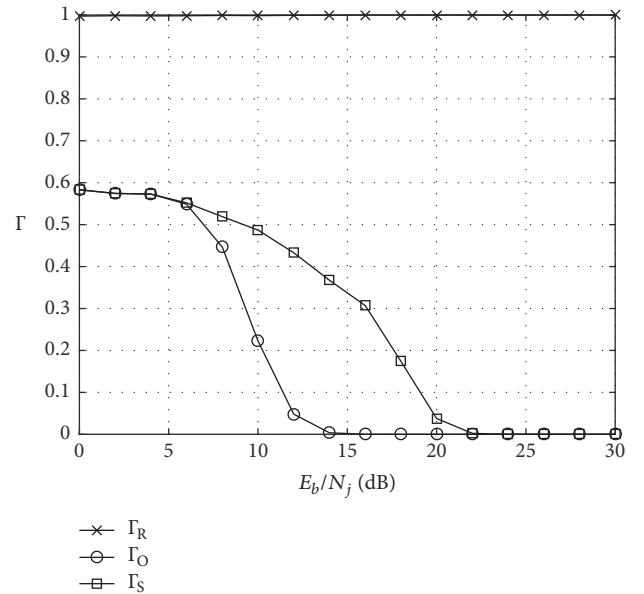


FIGURE 9: Trapped-error probability of various iterative schemes over partial-band jamming and Rayleigh fading channels with  $p = 0.3$ ,  $\rho = 0.1$ , and  $E_b/N_0 = 12$  dB.

discussed above, the fast decreasing trapped-error probability of the output measure causes the performance degradation of O-GMD decoding at approximately 10 dB in Figure 9.

## 6. Concluding Remarks

In this paper, we considered iterative erasure insertion and decoding schemes that do not require any preoptimized thresholds or any CSIR. Additionally, we proposed a new

analysis framework for the ratio, output, and sum measures. From the simulation results, we confirmed that the ratio-based GMD decoding scheme and its two-dimensional schemes have the best performance. Using the trapped-error probability, the performances of the iterative erasure insertion and decoding schemes are explained.

## Appendix

### Error and Erasure Probability of Sum Threshold Test

Let us denote the symbol error and erasure probabilities of STT as  $P_{\text{err}}$  and  $P_{\text{ers}}$ , respectively. The symbol error event occurs when a received symbol is erroneous but is not erased by STT. The symbol erasure event occurs when a received symbol is erased by STT. The two probabilities can be divided into two cases, as follows:

$$\begin{aligned} P_{\text{err}} &= (1 - \rho) P_{U,\text{err}} + \rho P_{J,\text{err}}, \\ P_{\text{ers}} &= (1 - \rho) P_{U,\text{ers}} + \rho P_{J,\text{ers}}, \end{aligned} \quad (\text{A.1})$$

where  $J$  and  $U$  refer to the jammed and the unjammed cases, respectively. We denote the symbol erase event of STT by  $H_s$ , that is,  $z = \sum_{j=0}^{M-1} y_j > \mu$ . Then,  $P_{U,\text{err}}$  can be represented as follows:

$$\begin{aligned} P_{U,\text{err}} &= \Pr [H_0, \bar{H}_s | U] \\ &= \Pr [\bar{H}_s | U] - \Pr [\bar{H}_0, \bar{H}_s | U]. \end{aligned} \quad (\text{A.2})$$

The first term,  $\Pr[\bar{H}_s | U]$ , and the second term,  $\Pr[\bar{H}_0, \bar{H}_s | U]$ , are given as (A.3) and (A.4), respectively. Similarly,  $P_{U,\text{ers}} = \Pr[H_s | U] = 1 - \Pr[\bar{H}_s | U]$  can be obtained using (A.3). By replacing  $g_{U,j}$  with  $g_{J,j}$ ,  $j = 0, \dots, M-1$ , we can calculate the error and erasure probabilities of the unjammed case. For the case in which a jamming signal exists,  $P_{J,\text{err}}$  and  $P_{J,\text{ers}}$  can be calculated by substituting  $g_{J,j}(y_j)$  for  $g_{U,j}(y_j)$ ,  $j = 0, \dots, M-1$ . The derivation of average error probability  $P_{\text{err}}$  and erasure probability  $P_{\text{ers}}$  is complete.

$$\Pr [\bar{H}_s | U] = \Pr [z < \mu | U] = \Pr \left[ \sum_{j=0}^{M-1} y_j < \mu \right] = \int_0^\mu \int_0^{\mu-y_0} \cdots \int_0^{\mu-\sum_{j=0}^{M-2} y_j} \prod_{j=0}^{M-1} g_{U,j}(y_j) dy_{M-1} \cdots dy_1 dy_0, \quad (\text{A.3})$$

$$\begin{aligned} \Pr [\bar{H}_0, \bar{H}_s | U] &= \Pr \left[ y_0 > y_j, \forall j = 1, \dots, M-1, \sum_{j=0}^{M-1} y_j < \mu \right] \\ &= \int_0^\mu \int_0^{\min(y_0, \mu-y_0)} \cdots \int_0^{\min(y_0, \mu-\sum_{j=0}^{M-2} y_j)} \prod_{j=0}^{M-1} g_{U,j}(y_j) dy_{M-1} \cdots dy_1 dy_0. \end{aligned} \quad (\text{A.4})$$

## Disclosure

The present address of Jinsoo Park is the Agency for Defense Development, Daejeon, Republic of Korea.

## Conflicts of Interest

The authors declare that they have no conflicts of interest.

## Acknowledgments

The authors gratefully acknowledge the support from Electronic Warfare Research Center at the Gwangju Institute of Science and Technology (GIST), originally funded by the Defense Acquisition Program Administration (DAPA) and the Agency for Defense Development (ADD).

## References

[1] L. Milstein and M. Simon, "Spread Spectrum Communications," in *The Mobile Communications Handbook, Second Edition*, vol. 19990749 of *Electrical Engineering Handbook*, CRC Press, 1999.

[2] C. W. Baum and M. B. Pursley, "Bayesian Methods for Erasure Insertion in Frequency-Hop Communication Systems with Partial-Band Interference," *IEEE Transactions on Communications*, vol. 40, no. 7, pp. 1231–1238, 1992.

[3] L.-L. Yang and L. Hanzo, "Performance analysis of coded M-ary orthogonal signaling using errors-and-erasures decoding over frequency-selective fading channels," *IEEE Journal on Selected Areas in Communications*, vol. 19, no. 2, pp. 211–221, 2001.

[4] A. J. Viterbi, "A Robust Ratio-Threshold Technique to Mitigate Tone and Partial Band Jamming in Coded MFSK Systems," in *Proceedings of the IEEE Military Communications Conference MILCOM 1982*, pp. 22.4-1–22.4-5, Boston, MA, October 1982.

[5] L.-L. Yang and L. Hanzo, "Low complexity erasure insertion in RS-coded SFH spread-spectrum communications with partial-band interference and nakagami-m fading," *IEEE Transactions on Communications*, vol. 50, no. 6, pp. 914–925, 2002.

[6] S. Ahmed, L.-L. Yang, and L. Hanzo, "Erasure insertion in RS-coded SFH MFSK subjected to tone jamming and Rayleigh fading," *IEEE Transactions on Vehicular Technology*, vol. 56, no. 6 I, pp. 3563–3571, 2007.

[7] H. A. Ngo, S. Ahmed, L.-L. Yang, and L. Hanzo, "Non-coherent cooperative communications dispensing with channel estimation relying on erasure insertion aided Reed-Solomon

- coded SFH M-ary FSK subjected to partial-band interference and Rayleigh fading,” *IEEE Transactions on Communications*, vol. 60, no. 8, pp. 2177–2186, 2012.
- [8] T. G. Macdonald and M. B. Pursley, “Staggered interleaving and iterative errors-and-erasures decoding for frequency-hop packet radio,” *IEEE Transactions on Wireless Communications*, vol. 2, no. 1, pp. 92–98, 2003.
- [9] C.-M. Lee, Y. T. Su, and L.-D. Jeng, “Performance analysis of block codes in hidden Markov channels,” *IEEE Transactions on Communications*, vol. 56, no. 1, pp. 1–4, 2008.
- [10] A. Aung, K. C. Teh, and K. H. Li, “Detection and countermeasure of interference in slow FH/MFSK systems over fading channels,” *Physical Communication*, vol. 10, pp. 11–23, 2014.
- [11] J. G. Kim, “Error and erasure decoding scheme for RS codes in MFSK based FH/SSMA communication,” *International Journal of Multimedia and Ubiquitous Engineering*, vol. 10, no. 10, pp. 11–20, 2015.
- [12] R. Koetter and A. Vardy, “Algebraic soft-decision decoding of Reed-Solomon codes,” *Institute of Electrical and Electronics Engineers Transactions on Information Theory*, vol. 49, no. 11, pp. 2809–2825, 2003.
- [13] J. Jiang and K. R. Narayanan, “Iterative soft decoding of Reed-Solomon codes,” *IEEE Communications Letters*, vol. 8, no. 4, pp. 244–246, 2004.
- [14] P. Sehier, P. Brelivet, and I. Aubry, “New jammer estimation method adapted to FH-PSK waveforms,” in *Proceedings of the 1994 IEEE MILCOM. Part 3 (of 3)*, pp. 1027–1031, October 1994.
- [15] M. Pursley and J. Skinner, “Decoding strategies for turbo product codes in frequency-hop wireless communications,” in *Proceedings of the IEEE International Conference on Communications*, pp. 2963–2968, Anchorage, AK, USA.
- [16] M. B. Pursley and J. S. Skinner, “Adaptive coding for frequency-hop transmission in mobile ad hoc networks with partial-band interference,” *IEEE Transactions on Communications*, vol. 57, no. 3, pp. 801–811, 2009.
- [17] M. R. Masse, M. B. Pursley, and J. S. Skinner, “Adaptive coding for frequency-hop transmission over fading channels with partial-band interference,” *IEEE Transactions on Communications*, vol. 59, no. 3, pp. 854–862, 2011.
- [18] H. El Gamal and E. Geraniotis, “Iterative channel estimation and decoding for convolutionally coded anti-jam FH signals,” *IEEE Transactions on Communications*, vol. 50, no. 2, pp. 321–331, 2002.
- [19] G. D. Forney, “Generalized Minimum Distance Decoding,” *IEEE Transactions on Information Theory*, vol. IT-12, no. 2, pp. 125–131, 1966.
- [20] D. Chase, “A Class of Algorithms for Decoding Block Codes with Channel Measurement Information,” *IEEE Transactions on Information Theory*, vol. 18, no. 1, pp. 170–182, 1972.
- [21] H. Tang, Y. Liu, M. Fossorier, and S. Lin, “On combining Chase-2 and GMD decoding algorithms for nonbinary block codes,” *IEEE Communications Letters*, vol. 5, no. 5, pp. 209–211, 2001.
- [22] S.-W. Lee and B. V. K. V. Kumar, “Soft-decision decoding of reed-solomon codes using successive error-and-ersure decoding,” in *Proceedings of the 2008 IEEE Global Telecommunications Conference, GLOBECOM 2008*, pp. 3065–3069, USA, December 2008.
- [23] E. R. Berlekamp, “Readable Erasures Improve the Performance of Reed-Solomon Codes,” *IEEE Transactions on Information Theory*, vol. 24, no. 5, pp. 632–633, 1978.
- [24] J. G. Proakis and M. Salehi, *Essentials of Communication Systems Engineering*, 2005.
- [25] W. G. Phoel, “Iterative demodulation and decoding of frequency-hopped PSK in partial-band jamming,” *IEEE Journal on Selected Areas in Communications*, vol. 23, no. 5, pp. 1026–1033, 2005.
- [26] S. Lin and D. J. Costello, *Error Control Coding*, Pearson, 2nd edition, 2004.
- [27] J. K. Wolf, A. M. Michelson, and A. H. Levesque, “On the Probability of Undetected Error for Linear Block Codes,” *IEEE Transactions on Communications*, vol. 30, no. 2, pp. 317–324, 1982.
- [28] A. Ramesh, A. Chockalingam, and L. B. Milstein, “Performance of noncoherent turbo detection on Rayleigh fading channels,” in *Proceedings of the IEEE Global Telecommunications Conference GLOBECOM’01*, pp. 1193–1198, USA, November 2001.
- [29] M. C. Valenti and S. Cheng, “Iterative demodulation and decoding of turbo-coded M-ary noncoherent orthogonal modulation,” *IEEE Journal on Selected Areas in Communications*, vol. 23, no. 9, pp. 1739–1747, 2005.
- [30] I. S. Gradshteyn and I. M. Ryzhik, *Table of Integrals, Series, and Products*, Academic Press, Boston, Mass, USA, 5th edition, 1994.





**Hindawi**

Submit your manuscripts at  
[www.hindawi.com](http://www.hindawi.com)

